

*Full Length Research Paper*

# Frictional effect on stress and displacement fields in contact region

Saeed Adibnazari and Ali Anvari\*

Department of Mechanical and Aerospace Engineering, Science and Research Branch, Islamic Azad University, Tehran, Iran.

Received 6 August, 2017; Accepted 7 September, 2017

In this study, by applying Giannakopoulos and Pallot's stress and displacement equations, and using the Goryacheva's friction model, the stress and displacement equations are obtained. Finally, by applying analytical method, these equations are solved. By assuming that the roller is rigid and the substrate is almost homogeneous with constant Poisson ratio and constant elastic modulus, the results of frictional effect on stress and displacement fields are achieved and are shown in figures. Using different amounts of friction coefficient, the effect of friction coefficient on stress and displacement inside the contact region in the figures is observed. The new results achieved by the analytical method used in this study for obtaining tangential stress and displacement inside the contact region is compared with the results that were already achieved for obtaining tangential stress and displacement inside the contact region in another study. The comparison between the two analytical methods showed similarity in the results that are achieved by both methods. These results may be very advantageous in the design of suitable substrate and cylinder that are in contact, especially in the model that the substrate is almost homogeneous and the cylinder is rigid.

**Key words:** Friction, contact, stress field, displacement field.

## INTRODUCTION

The present study examines the frictional effect on stress and displacement fields in the contact region. It appears that friction is an undeniable phenomenon in contact with two or more materials. For calculating the amount of friction, many approaches are employed. One of the important contacts investigated in the presence of friction is the contact of roller with half space. Wheel with rail, as well as tire with road, contacts are examples of roller contact with half space. The contact region is the region

where two or more materials are in contact and can be divided into three zones, viz; slip zone, partial slip zone, and stick zone. In a contact region, there is a possibility of the existence of one or more stick or slip zones.

It appears that friction can be very effective on stress and displacement fields and can cause increase and decrease in the stress and displacement amounts in contact region. Thus, the aim of this study is to investigate the frictional effect on stress and

\*Corresponding author. E-mail: alianvari330@yahoo.com.

displacement fields because the numerical values of stress and displacement are required for selecting the contacting materials, since each contacting materials have specific friction coefficient. As a result, by selecting a material with suitable friction coefficient, the stress and displacement amounts may be controlled.

The method of complex variables developed by Muskhelishvili (1949), Galin (1953) and Kalandiya (1975) is mainly used to determine the stress distribution for the 2-D contact problems in the presence of friction. The linear form of the friction law is normally used in the problem formulations (Goryacheva, 1998).

Initial studies on the contact between two bodies took place near the end of the nineteenth century by German researcher, Heinrich Hertz (Hertz, 1882). An English researcher Carter, in the late nineteen-twenties was the first to evaluate the tangential forces between two rolling bodies (Carter, 1926). He aimed to evaluate locomotive railroad wheels in contact with the rail, considering only the longitudinal creep, and found the tangential forces in that direction. He was also the first to propose a model that considers the creep in the longitudinal direction. In addition, Johnson generalized Carter's results to circular contacts as well as longitudinal and lateral creep (Johnson, 1958). Vermeulen and Johnson (1964) generalized this theory to elliptical contact areas. All of this work is Hertzian-based, giving contact solutions for a class of geometrical objects satisfying the half-space restriction (Vermeulen and Johnson, 1964).

Also, in 1949, M'Ewen evaluated the contact between two cylinders and calculated the stress field, taking into account the tangential load due to the friction on the contact area. His study was the first to include friction force on the model (M'Ewen, 1949). In the early nineteen-sixties, Haines and Ollerton (1963) came up with an approximated solution for shear stress distribution in an elliptic contact area. They also compared their results with photo elasticity experiments and found good agreement (Haines and Ollerton, 1963). Furthermore, in the late nineteen-sixties, Kalker (1967) presented his Ph.D. thesis in which he proposed a new revolutionary theory for contact between rolling bodies. He calculated all tangential forces and creep coefficients and also found the rigidity parameters involved in the analysis. His work, also based on the Hertz Theory, was used to develop several simplified algorithms (Fastism) and complete programs (Contact) to calculate the forces in the contact. His research provided an outstanding contribution to railroad research, because his theory explained and enabled the calculation of several parameters used in the wheel-rail modeling, like creep, yaw angle, spin and others (Kalker, 1967).

Sackfield and Hills (1983) put together the existing theories for circular and rectangular contact areas. They considered both the longitudinal and tangential loads and proposed a model to obtain the stress field for both cases, with each one identified using the axle ratio,  $k$ .

The results obtained were similar to the ones calculated by other researchers before them (Sackfield and Hills, 1983). In addition, the theories: Linear theory, Simplified theory, Empirical theory, Strip theory and Exact three-dimensional rolling contact theory assume that the contact between the two bodies is non-conformal. Li and Kalker (1998) introduced an approach for numerical solution of the conformal contact between the wheel and the rail. Moreover, in 2000, Giannakopoulos and Pallot examined two-dimensional contact of a rigid cylinder on an elastic graded substrate. The normal, sliding and rolling types of contact along with effect of adhesion in frictionless contact are addressed and examined in this paper. The elastically graded substrate is modeled to be locally isotropic with constant Poisson ratio and elastic modulus that varies with depth,  $y$ , according to a power law,  $E = E_0 y^k$ ;  $0 \leq k < 1$ ,  $y \geq 0$ . Such variation covers a fairly broad class of graded materials. Exact results are derived within the context of small deformation linear elasticity. The results show that the power law elastic gradation can be very advantageous in the design of strong and wear resistance sliding surfaces (Giannakopoulos and Pallot, 2000). Furthermore, Santos et al. (2004) evaluated the stress field inside elastic rolling bodies with an ellipse area of contact. This kind of model can be applied to wheel-rail contact phenomena.

Also, Ke and Wang (2010) investigated the partial slip contact problem of two functionally graded material (FGM) coating/substrate systems by employing the Goodman approximation. The stress analysis showed that the FGM coating reduces the interface stress concentration that arises due to the elastic constant mismatch (Ke and Wang, 2010). In addition, in 2011, Ruderman and Bertram presented Modified Maxwell-slip model of pre-sliding friction (Ruderman and Bertram, 2011). An enhanced friction modeling for steady-state rolling tires is proposed by Rene van der Steen. In his modeling he proposed a friction coefficient model as a function of sliding velocity in a contact of cylinder with half space (Steen, 2010).

The tractive rolling contact problem between a rigid cylinder and a graded coating is investigated by Guler et al. (2011). The main objective of this study is to investigate the effect of the stiffness ratio, the coefficient of friction and the coating thickness on the surface contact tractions, the surface in-plane stress, the stick zone length and the creep ratio parameter that may have a bearing on the fatigue life of the component. Assuming that the shear modulus varies exponentially through the thickness of the coating, the governing integral equations associated with the rolling contact problem is constructed. Furthermore, it is supposed that the contact patch is controlled by a central stick zone accompanied by two slip zones. The conventional Goodman approximation is employed in order to decouple the governing singular integral equations. Finally, the numerical solution of the integral equations is obtained by

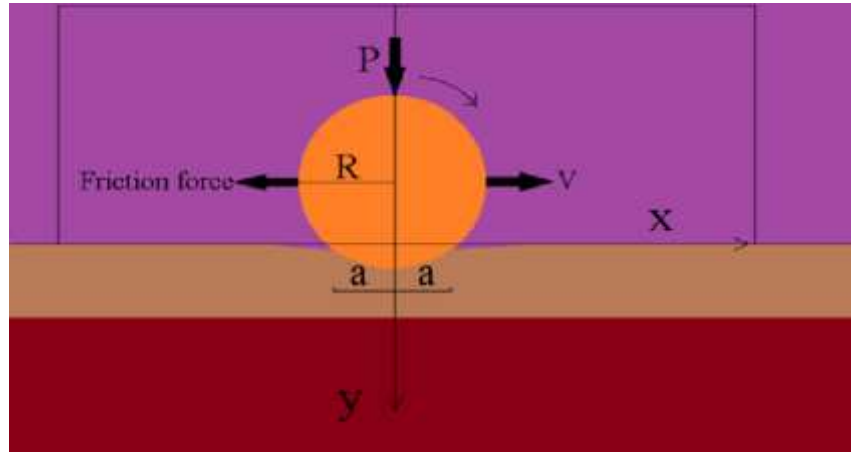


Figure 1. Coordinates system that is assumed in contact of roller with half space.

applying the Gauss-Chebyshev integration method (Guler et al., 2011).

Furthermore, in the area of obtaining analytical evaluation methods for determining mechanical properties of different materials, a few works are submitted by Anvari (2014, 2016a, 2016b, 2017, 2017a, 2017b, 2017c,). Moreover, in the area of contact mechanics, a few publications are presented by Areias et al. (2014, 2015) and Timon and Huilong (2017).

As it appears, many efforts have been made in the field of contact mechanics to develop the equations for obtaining stress and displacement amounts inside the contact region, but the exact consideration of the relation between the friction and stress fields, and the relation between the friction and displacement fields in different contact zones like, slip and stick zones in contact of roller with a half space, is still required.

In the present research, the frictional effect on stress and displacement fields for contact of roller with half space is investigated. As mentioned in the study, the results shown in the figures, indicate the relation between the stress and friction coefficient and the relation between the displacement and friction coefficient inside the contact region. Since the amounts of stress and displacement are required in many of the proper designs, these results may be used in designing process of solid mechanics.

**PROBLEM FORMULATION**

**Friction model**

In order to describe the friction model and associated stress in the contact region, some assumptions are required to be considered. These assumptions are defined by Goryacheva (1998) and Giannakopoulos and Pallot (2000). Definition of this method may contribute to the explanation of the equations in friction model that determine the relation between normal and tangential load, etc.

“For a contact of roller with half space, if a tangential force Q

applied to the body satisfies the inequality  $Q < \mu P$ , where P is the normal force and  $\mu$  is the friction coefficient, then partial slip occurs; this is characterized by the friction. If  $Q = \mu P$ , there is limiting friction, and the condition of full slip occurs in the contact region. This case is also called sliding friction. The case  $Q = 0$  corresponds to pure rolling” (Goryacheva, 1998). In Figures 1 and 2 the contact between rigid roller with half space under the normal load P is shown. In Figure 1, Q is the tangential load, a is the half of the contact length, R is the cylinder radius, and v is the velocity in x direction.

“For cylinder in rolling contact under normal load with torque transmission, slipping may take place over part of the contact where the limiting value of traction is reached, while over the rest of the contact area (where the tangential traction is less than the limiting value), the contacting surfaces are locked and no slipping takes place” (Giannakopoulos and Pallot, 2000). In Figure 3, tangential and normal stress in contact of roller with half space is illustrated.

**Muskhelishvili method**

One of the attempts that is performed in order to obtain stress inside the contact region is mechanics of elastic contacts (Hills et al., 1993). In this method, the Muskhelishvili potential function is applied to obtain stress inside the contact region. Whereas Equation 1 is the Muskhelishvili potential function, Equation 2 is the Muskhelishvili potential function by taking the conjugate of both sides. Equations 3, 4, and 5 are the equations to obtain stress inside the contact region. In the following equations, z is a complex variable, f is friction coefficient, and P(x) is the function of normal load in contact region. In Figure 4,  $p_0$  is the normal load in unit of length and q is the tangential load in unit of length inside the contact region.

$$\phi(z) = \frac{1-if}{2\pi i} \int \frac{P(x)}{x-z} dx = -\frac{(i+f)}{2\pi} \int \frac{P(x)}{x-z} dx \tag{1}$$

$$\bar{\phi}(z) = -\left(\frac{1+if}{1-if}\right) * \phi(z) \tag{2}$$

$$\sigma_{xx} + \sigma_{yy} = 2[\phi(z) + \bar{\phi}(z)] \tag{3}$$

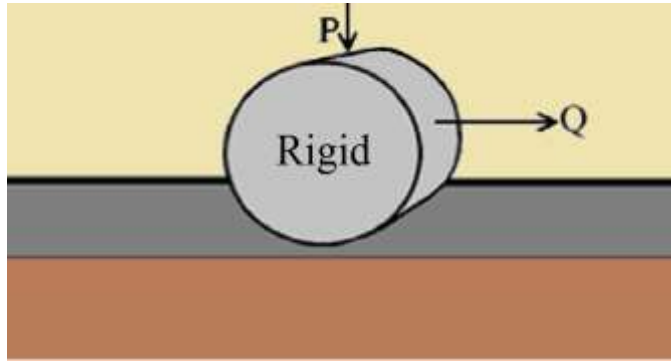


Figure 2. The contact of rigid cylinder with substrate.

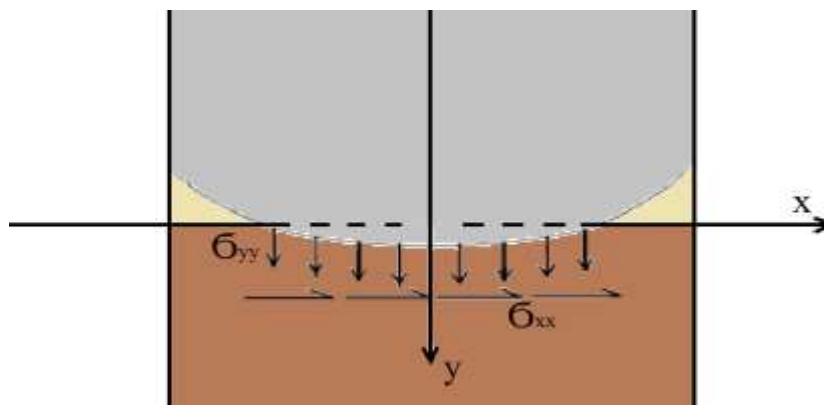


Figure 3. Tangential and normal stress in contact of roller with half space.

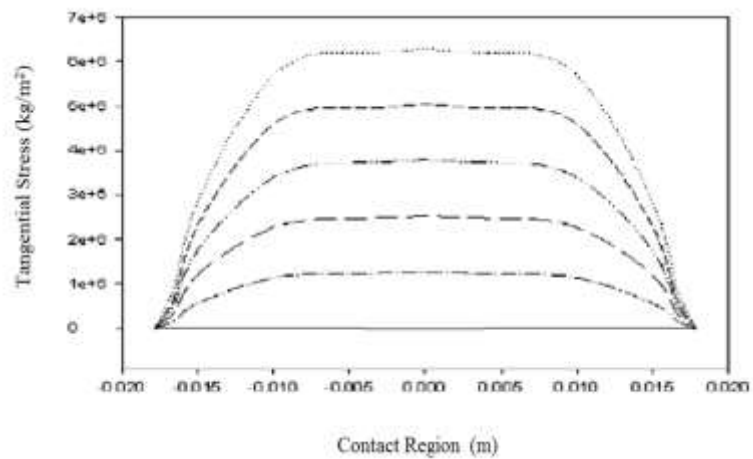
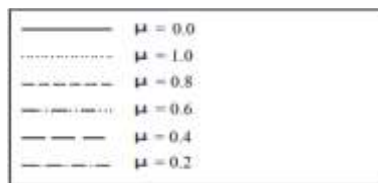


Figure 4. Tangential stress inside the contact region.

**Table 1.** Numerical values of parameters and unknown quantities used to obtain stress and displacement inside the contact region of roller with half space.

No. 1	No. 2	No. 3	No. 4	No. 5	No. 6	No. 7	No. 8	No. 9	No. 10
v	E <sub>0</sub> (kg/m <sup>2</sup> )	l <sub>k</sub>	J <sub>k</sub>	β	k	h (m)	a (m)	Γ	R (m)
0.3	1767600	0.3489	0.3255	1.0261	0.1	0.0053	0.0178	1	0.3

$$\sigma_{yy} - \sigma_{xx} + 2i\tau xy = 2[(\bar{z} - z)(\partial \phi(z) / \partial x) - \bar{\phi}(z) - \phi(z)], \tag{4}$$

$$\sigma_{xx} = 2 \left[ \phi(z) - \frac{1+if}{1-if} \phi(z) \right] \tag{5}$$

By substituting the Muskhelishvili potential function (Equation 1) in Equation 5, Equation 6 is obtained.

$$\sigma_{xx} = 2 \left[ \frac{(i+f)}{2\pi} \int \frac{P(x)}{x-z} dx - \frac{1+if}{1-if} * \left( \frac{(i+f)}{2\pi} \int \frac{P(x)}{x-z} dx \right) \right] \tag{6}$$

Also, by following the solution method, there is:

$$\sigma_{xx} = \left[ \frac{(-i-f)*(1-if) + (1+if)*(i+f)}{\pi(1-if)} \right] \int \frac{P(x)}{x-z} dx, \tag{7}$$

$$\sigma_{xx} = \left[ \frac{-i-f-f+i(f*f) + 1+i-f-f+i(f*f)}{\pi(1-if)} \right] \int \frac{P(x)}{x-z} dx, \tag{8}$$

$$\sigma_{xx} = \frac{-2f + 2i(f*f)}{\pi(1-if)} \int \frac{P(x)}{x-z} dx, \tag{9}$$

$$\sigma_{xx} = \frac{2\sqrt{(-f)^2 + (f^2)^2} * e^{i \arctan(-f)}}{\pi\sqrt{1+f^2} * e^{i \arctan(-f)}} \int \frac{P(x)}{x-z} dx, \tag{10}$$

Finally, by solving Equation 10, Equation 11 for the tangential stress inside the contact region is obtained.

$$\sigma_{xy} = \frac{2\sqrt{(-f)^2 + (f^2)^2}}{\pi\sqrt{1+f^2}} \int \frac{P(x)}{x-z} dx \tag{11}$$

In Muskhelishvili's closed-form expression (Hills et al., 1993), the tangential stress in unit of length inside the partial slip contact region is indicated. Muskhelishvili's closed-form expression involves the tangential stress in contact region in unit of length of cylinder with substrate (Hills et al., 1993). In this expression, the points 1 to 12 will be used to compare the results of this study (Figure 7) and the results of the book (Hills et al., 1993).

**Giannakopoulos and Pallot's method**

Here, the parameters and variables that are used in Giannakopoulos and Pallot's method to obtain stress and displacement inside the contact region are introduced. Furthermore, the method to solve the Giannakopoulos and Pallot's stress

equations are explained.

In Equation 12, Γ is a function that defines the substrate stiffness ratio (Guler et al., 2011). The substrate is assumed almost homogeneous and its stiffness is constant, therefore Γ = 1. In Equation 13, v is the Poisson ratio and in the following equations β, l<sub>k</sub>, k, and J<sub>k</sub> are the parameters reflecting the material properties of the substrate. In the homogeneous limit, k→0, and in the elastic limit, k→1 (Giannakopoulos and Pallot, 2000). As mentioned in the previous paragraph, because the substrate is almost homogeneous, k = 0.1.

$$l_k = \frac{\pi * \Gamma(3+k)}{2^{(k+2)}(k+2)\Gamma\left(\frac{3+k+\beta}{2}\right)\Gamma\left(\frac{3+k-\beta}{2}\right)} \tag{12}$$

$$\beta = \beta(v, k) = \sqrt{(k+1)\left(1 - \frac{kv}{1-v}\right)} \tag{13}$$

$$J_k = \frac{\beta}{(k+1)} l_k \tag{14}$$

In Equation 15, R is the radius of cylinder, P is the normal load, and E<sub>0</sub> is the substrate elastic modulus. In Equation 16, h is the indentation of cylinder into the substrate, whereas a is the half of the contact length in contact of cylinder with substrate (Giannakopoulos and Pallot, 2000).

$$a^{(2+k)} = \frac{(1-v^2)2RP\beta(k+2)\sin(\beta\pi/2)}{E_0(1-k^2)\pi} \Gamma\left(\frac{3+k+\beta}{2}\right) \Gamma\left(\frac{3-k}{2}\right) \Gamma\left(\frac{3+k}{2}\right) \tag{15}$$

$$h = \frac{a^2}{2Rk} \tag{16}$$

In this study, the numerical values indicated in Table 1 are used for different parameters and unknown quantities. All the numerical values in order to obtain the stress are available in Table 1. Only by having the stress equations and substituting the above numerical values in the stress equations can they be obtained. It is noticeable that the aim is to obtain the frictional effect on stress fields. So by changing the μ in stress equations, the frictional effect on stress fields can be achieved. Equation 17 illustrates a stress equation that is dependent on friction coefficient.

$$\sigma_{xx}(x, y) = -\frac{P}{2I_k} \int_{-a}^a \frac{y^3(x-s)^2 \cos[\beta \arctan((x-s)/y)]}{[(x-s)^2 + y^2]^{(3+k)/2}} ds - \frac{\mu P}{2J_k} \int_{-a}^a \frac{y^3(x-s)^2 \sin[\beta \arctan((x-s)/y)]}{[(x-s)^2 + y^2]^{(3+k)/2}} ds, \tag{17}$$

From Equation 17, by using the partial integral solution method, the

numerical values mentioned in Table 1, assuming  $h = y = 0.0053$  m, and substituting the numerical values of  $x$  between the range 0.0178 m to 0.0178 m ( $-a, a$ ) may be solved.

**Stress equation solution method**

The assumption of Goryacheva  $Q = \mu P$ , means that in stress equations,  $\mu P$  instead of  $Q$  can be substituted. Thus, stress equation that is dependent on friction coefficient may be obtained. In this method, by changing the numerical value of  $\mu$  in the range,  $0 < \mu < 1$ , in stress equations, the effect of friction coefficient on stress inside the contact region of roller with half space can be achieved. In order to explain the solution method, the following procedure is explained. The following equation is the stress equation in  $x$  direction.

$$\sigma_{xx}(x, y) = -\frac{P}{2J_k} \int_{-a}^a \frac{y^k(x-s)^2 \cos[\beta \arctan((x-s)/y)]}{[(x-s)^2 + y^2]^{(3+k)/2}} ds - \frac{Q}{2J_k} \int_{-a}^a \frac{y^k(x-s)^2 \sin[\beta \arctan((x-s)/y)]}{[(x-s)^2 + y^2]^{(3+k)/2}} ds \tag{18}$$

By substituting  $\mu P$  instead of  $Q$  in Equation 18, Equation 19 is obtained.

$$\sigma_{xx}(x, y) = -\frac{P}{2J_k} \int_{-a}^a \frac{y^k(x-s)^2 \cos[\beta \arctan((x-s)/y)]}{[(x-s)^2 + y^2]^{(3+k)/2}} ds - \frac{\mu P}{2J_k} \int_{-a}^a \frac{y^k(x-s)^2 \sin[\beta \arctan((x-s)/y)]}{[(x-s)^2 + y^2]^{(3+k)/2}} ds \tag{19}$$

It can be observed that Equation 19 is dependent on  $\mu$ , and with changing  $\mu$ ,  $S_{xx}$  changes, which is the aim of this study; the effect of friction on stress field. By substituting  $\mu P$  instead of  $Q$  in stress equations  $S_{yy}$  and  $S_{xy}$ , the exact same thing occurred. It is noticeable that in this solution for stress equations, only the first two partial integrals terms are used. Using more than two partial integrals terms in the solution of the stress integral equations is not necessary.

$$\sigma_{xx}(x, y) = -\frac{P}{2J_k} \int_{-a}^a \frac{y^k(x-s)^2 \cos[\beta \arctan((x-s)/y)]}{[(x-s)^2 + y^2]^{(3+k)/2}} ds - \frac{Q}{2J_k} \int_{-a}^a \frac{y^k(x-s)^2 \sin[\beta \arctan((x-s)/y)]}{[(x-s)^2 + y^2]^{(3+k)/2}} ds \tag{20}$$

By substituting  $\mu P$  instead of  $Q$  in stress equation, and by applying the partial integral solution method, the tangential stress integral equation is solved and is shown in Equation 21.

$$\sigma_{xx}(x, y) = -\frac{Py^k}{2J_k} \left\{ \left[ (x-s) \cos[\beta \arctan((x-s)/y)] \right]^* \frac{[(x-s)^2 + y^2]^{-(3+k)/2+1}}{[-((3+k)/2)+1](-2)} \right. \\ \left. - \left[ \frac{-2 \cos[\beta \arctan((x-s)/y)] + \beta y \sin[\beta \arctan((x-s)/y)](x-s)}{[y^2 - (x-s)^2]^2} \right]^* \frac{[(x-s)^2 + y^2]^{-(3+k)/2+2}}{4[-((3+k)/2)+1][-(3+k)/2+2](x-s)} \right. \\ \left. - \frac{\mu Py^k}{2J_k} \left\{ \left[ (x-s) \sin[\beta \arctan((x-s)/y)] \right] \frac{[(x-s)^2 + y^2]^{-(3+k)/2+1}}{-2[-(3+k)/2+1]} \right. \right. \\ \left. \left. - \left[ -2 \sin[\beta \arctan((x-s)/y)] - \frac{\beta y \cos[\beta \arctan((x-s)/y)](x-s)}{y^2 - (x-s)^2} \right]^* \frac{[(x-s)^2 + y^2]^{-(3+k)/2+2}}{4[-((3+k)/2)+1][-(3+k)/2+2](x-s)} \right\} \right. \\ \left. \right\} \tag{21}$$

$$\sigma_{yy}(x, y) = -\frac{P}{2J_k} \int_{-a}^a \frac{y^{(2+k)} \cos[\beta \arctan((x-s)/y)]}{[(x-s)^2 + y^2]^{(3+k)/2}} ds - \frac{Q}{2J_k} \int_{-a}^a \frac{y^{(2+k)} \sin[\beta \arctan((x-s)/y)]}{[(x-s)^2 + y^2]^{(3+k)/2}} ds \tag{22}$$

By substituting  $\mu P$  instead of  $Q$  in stress equation, and by applying the partial integral solution method, the normal stress integral equation is solved and is shown in Equation 23.

$$\sigma_{yy}(x, y) = -\frac{Py^{(2+k)}}{2J_k} \left\{ \left[ \cos[\beta \arctan((x-s)/y)] \frac{[(x-s)^2 + y^2]^{-(3+k)/2+1}}{[-((3+k)/2)+1](-2)(x-s)} \right. \right. \\ \left. \left. - \left[ \frac{\beta y}{y^2 - (x-s)^2} \sin[\beta \arctan((x-s)/y)] \frac{[(x-s)^2 + y^2]^{-(3+k)/2+2}}{4[-((3+k)/2)+1][-(3+k)/2+2](x-s)^2} \right]^* \right. \right. \\ \left. \left. - \frac{\mu Py^{(2+k)}}{2J_k} \left\{ \left[ \sin[\beta \arctan((x-s)/y)] \frac{[(x-s)^2 + y^2]^{-(3+k)/2+1}}{[-(3+k)/2+1](-2)(x-s)} \right. \right. \right. \right. \\ \left. \left. \left. + \left[ \frac{\beta y \cos[\beta \arctan((x-s)/y)]}{y^2 - (x-s)^2} \frac{[(x-s)^2 + y^2]^{-(3+k)/2+2}}{4[-((3+k)/2)+1][-(3+k)/2+2](x-s)^2} \right]^* \right. \right. \right. \right. \\ \left. \left. \left. \right\} \right. \right. \\ \left. \right\} \tag{23}$$

$$\sigma_{xy}(x, y) = -\frac{P}{2J_k} \int_{-a}^a \frac{y^{(1+k)}(x-s) \cos[\beta \arctan((x-s)/y)]}{[(x-s)^2 + y^2]^{(3+k)/2}} ds - \frac{Q}{2J_k} \int_{-a}^a \frac{y^{(1+k)}(x-s) \sin[\beta \arctan((x-s)/y)]}{[(x-s)^2 + y^2]^{(3+k)/2}} ds \tag{24}$$

By substituting  $\mu P$  instead of  $Q$  in stress equation, and by applying the partial integral solution method, the shear stress integral equation is solved and is also shown in Equation 25.

$$\sigma_{xy}(x, y) = -\frac{Py^{(1+k)}}{2J_k} \left\{ \left[ \cos[\beta \arctan((x-s)/y)] \frac{[(x-s)^2 + y^2]^{-(3+k)/2+1}}{[-((3+k)/2)+1](-2)} \right. \right. \\ \left. \left. - \left[ -\cos[\beta \arctan((x-s)/y)] + \frac{y\beta \sin[\beta \arctan((x-s)/y)](x-s)}{[y^2 - (x-s)^2]} \right]^* \frac{[(x-s)^2 + y^2]^{-(3+k)/2+2}}{4[-((3+k)/2)+1][-(3+k)/2+2](x-s)^2} \right. \right. \\ \left. \left. - \frac{\mu Py^{(1+k)}}{2J_k} \left\{ \left[ \sin[\beta \arctan((x-s)/y)] \frac{[(x-s)^2 + y^2]^{-(3+k)/2+1}}{[-(3+k)/2+1](-2)} \right. \right. \right. \\ \left. \left. \left. - \left[ -\sin[\beta \arctan((x-s)/y)] - \frac{y\beta \cos[\beta \arctan((x-s)/y)](x-s)}{[y^2 - (x-s)^2]} \right]^* \frac{[(x-s)^2 + y^2]^{-(3+k)/2+2}}{4[-((3+k)/2)+1][-(3+k)/2+2](x-s)^2} \right. \right. \right. \right. \\ \left. \left. \left. \right\} \right. \right. \\ \left. \right\} \tag{25}$$

Figure 7 is used to prove that the method is used in this study seems correct, because Figure 7 has results similar to Muskhelishvili's closed-form expression.

**Displacement equation solution method**

Since all stress equations are solved and the results are observable in Figures 5 to 8, the displacement equations that are dependent on stress can be solved. In this part of study, the method that is used to solve the displacement equations is explained, and finally the results that are obtained by using the numerical values of Table 1 are shown in Figures 9 and 10. Finally, the displacement results that are obtained in this study are compared with the results that are already obtained by another analytical method. The equation for substrate tangential displacement is:

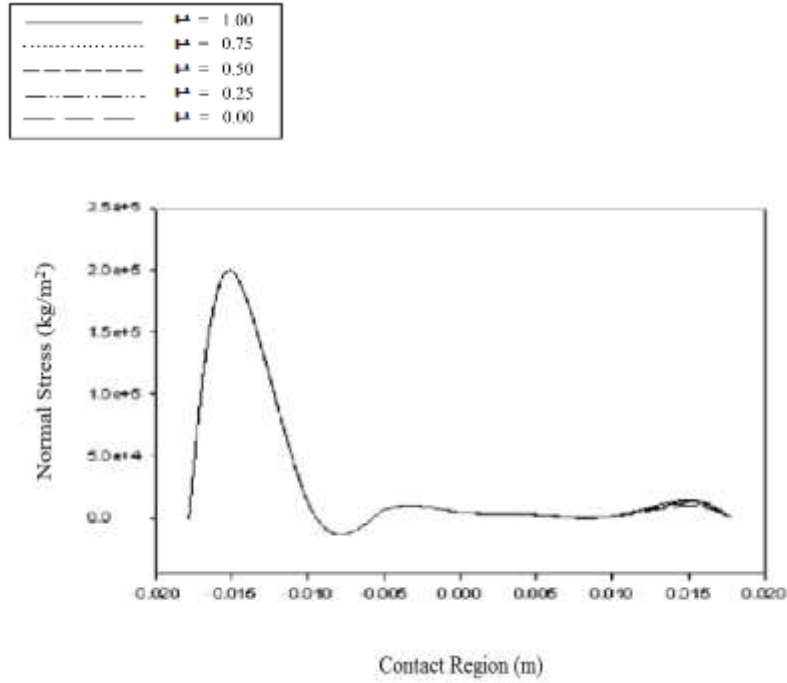


Figure 5. Normal stress inside the contact region.

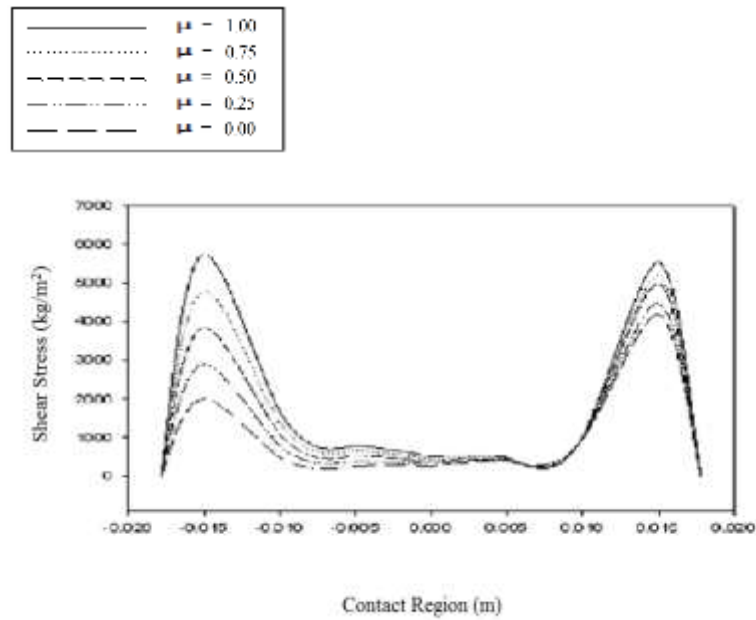


Figure 6. Shear stress inside the contact region.

$$u_y(x) = -\frac{(1-\nu^2)\cos(\beta\pi/2)}{E_0 2J_2} \left( \int_{-a}^a \frac{\sigma_{yy}}{k(x-s)^2} ds - \int_s^a \frac{\sigma_{yy}}{k(s-x)^2} ds \right) + \frac{(1-\nu^2)\sin(\beta\pi/2)}{E_0 2J_2} \int_{-a}^a \frac{\sigma_{xx}}{k|x-s|^2} ds. \quad (26)$$

$$u_y(x) = \frac{(1-\nu^2)\beta\cos(\beta\pi/2)}{E_0(k+1)2J_2} \left( \int_{-a}^a \frac{\sigma_{xx}}{k(x-s)^2} ds - \int_s^a \frac{\sigma_{xx}}{k(s-x)^2} ds \right) + \frac{(1-\nu^2)\beta\sin(\beta\pi/2)}{E_0(k+1)2J_2} \int_{-a}^a \frac{\sigma_{yy}}{k|x-s|^2} ds. \quad (27)$$

Furthermore, equation for normal displacement of substrate is:

By substituting the amounts of  $S_{xx}$  and  $S_{yy}$  in the Equation 26

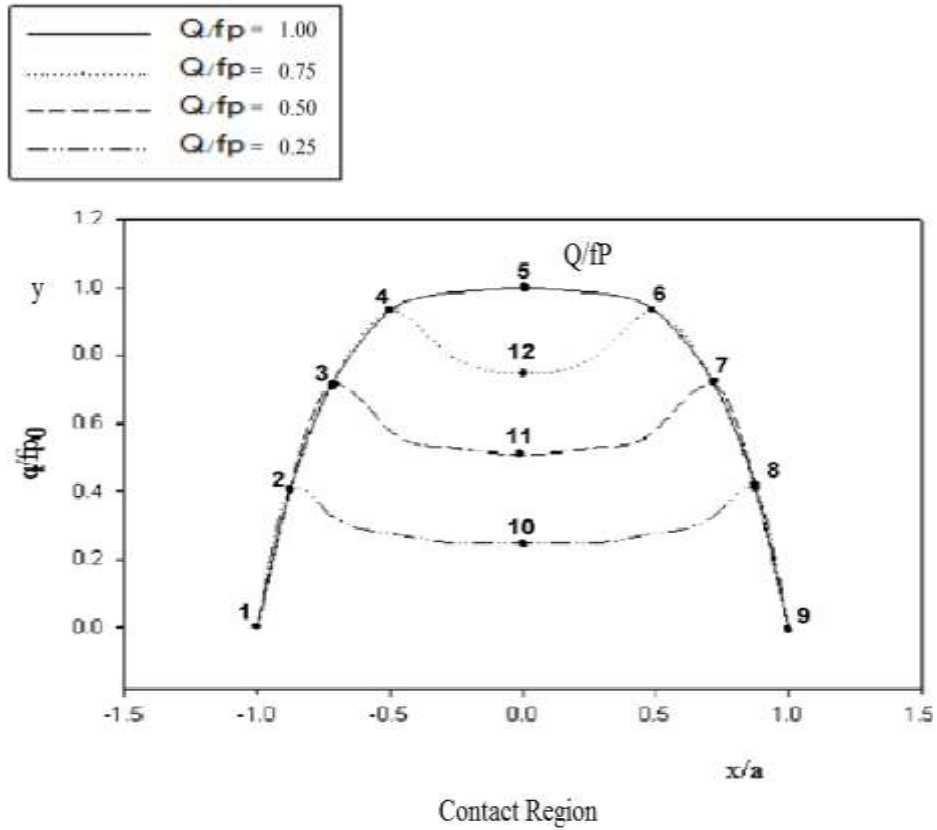


Figure 7. Tangential stress inside the partial slip contact region.

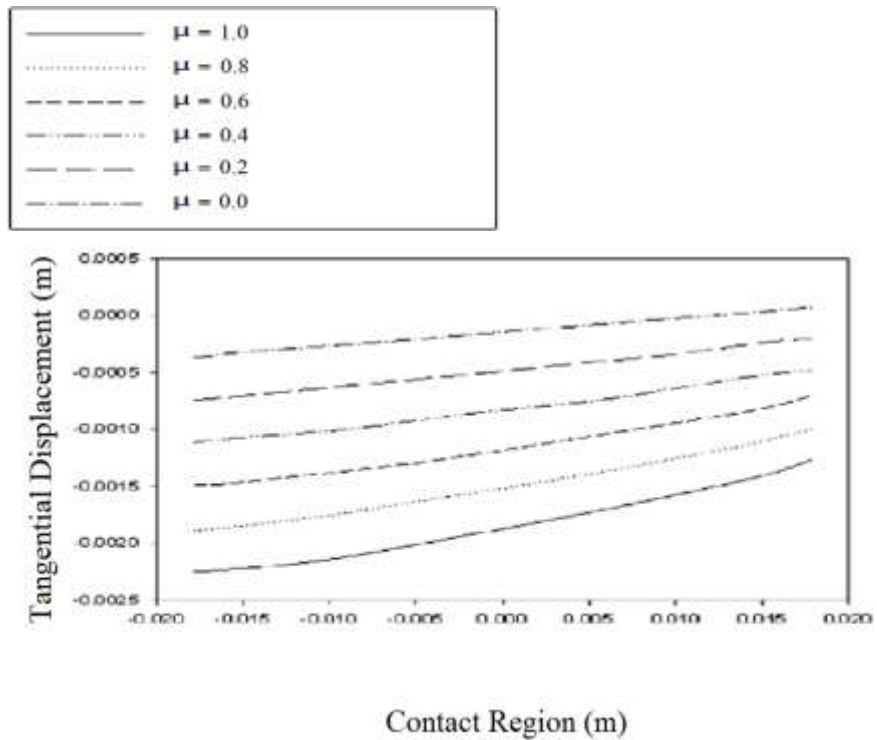


Figure 8. The tangential displacement in contact region.

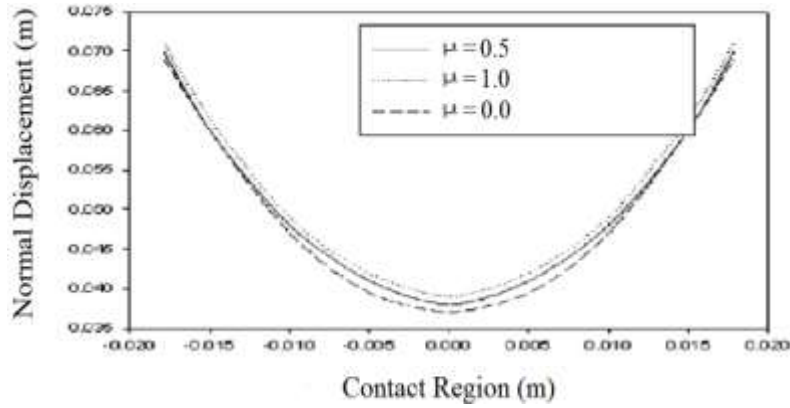


Figure 9. The normal displacement in contact region.

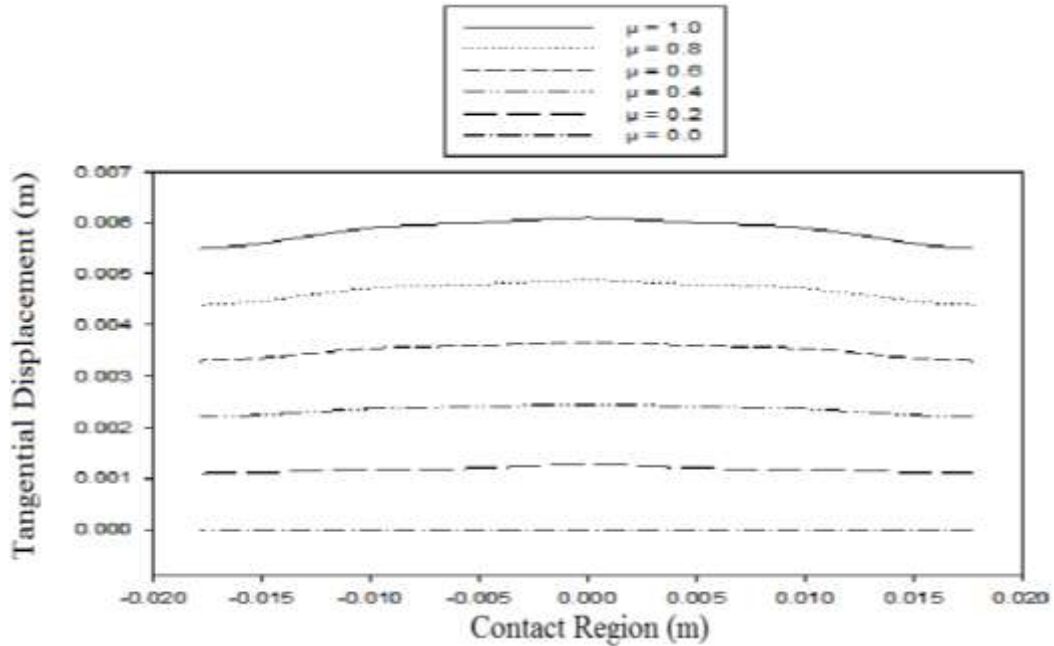


Figure 10. Tangential displacement inside the contact region.  
Source: Giannakopoulos and Pallot (2000).

and applying partial integral solution method to solve the tangential displacement integral equation, Equation 28 is obtained.

$$\begin{aligned}
 u_s(x) = & -\frac{(1-\nu^2)\cos(\beta\pi/2)}{E_s k 2J_s} \\
 & \left\langle \frac{-p(s)(x-s)^{-k+1}}{-k+1} - \frac{(\partial p(s)/\partial s)(x-s)^{-k+2}}{(-k+1)(-k+2)} + \frac{(\partial^2 p(s)/\partial s^2)(x-s)^{-k+3}}{(-k+1)(-k+2)(-k+3)} \right\rangle_s \\
 & - \left\langle \frac{p(s)(x-s)^{-k+1}}{-k+1} - \frac{(\partial p(s)/\partial s)(x-s)^{-k+2}}{(-k+1)(-k+2)} + \frac{(\partial^2 p(s)/\partial s^2)(x-s)^{-k+3}}{(-k+1)(-k+2)(-k+3)} \right\rangle_s \\
 & + \frac{(1-\nu^2)\sin(\beta\pi/2)}{E_s k 2J_s} \\
 & \left\langle \frac{q(s)|x-s|^{-k+1}}{-k+1} - \frac{(\partial q(s)/\partial s)|x-s|^{-k+2}}{(-k+1)(-k+2)} + \frac{(\partial^2 q(s)/\partial s^2)|x-s|^{-k+3}}{(-k+1)(-k+2)(-k+3)} \right\rangle_s
 \end{aligned} \tag{28}$$

In addition, Equation 28 is equal to

$$\begin{aligned}
 & -\frac{(1-\nu^2)\cos(\beta\pi/2)}{E_s k 2J_s} \\
 & \left( \left( \frac{-p(-a)(x+a)^{-k+1}}{-k+1} - \frac{(\partial p(-a)/\partial s)(x+a)^{-k+2}}{(-k+1)(-k+2)} + \frac{(\partial^2 p(-a)/\partial s^2)(x+a)^{-k+3}}{(-k+1)(-k+2)(-k+3)} \right) - \right. \\
 & \left. \left( \frac{p(a)(a-x)^{-k+1}}{-k+1} - \frac{(\partial p(a)/\partial s)(a-x)^{-k+2}}{(-k+1)(-k+2)} + \frac{(\partial^2 p(a)/\partial s^2)(a-x)^{-k+3}}{(-k+1)(-k+2)(-k+3)} \right) \right) \\
 & + \frac{(1-\nu^2)\sin(\beta\pi/2)}{E_s k 2J_s} \\
 & \left( \left( \frac{q(a)|x-a|^{-k+1}}{-k+1} - \frac{(\partial q(a)/\partial s)|x-a|^{-k+2}}{(-k+1)(-k+2)} + \frac{(\partial^2 q(a)/\partial s^2)|x-a|^{-k+3}}{(-k+1)(-k+2)(-k+3)} \right) \right. \\
 & \left. - \left( \frac{q(-a)|x+a|^{-k+1}}{-k+1} - \frac{(\partial q(-a)/\partial s)|x+a|^{-k+2}}{(-k+1)(-k+2)} + \frac{(\partial^2 q(-a)/\partial s^2)|x+a|^{-k+3}}{(-k+1)(-k+2)(-k+3)} \right) \right)
 \end{aligned} \tag{29}$$

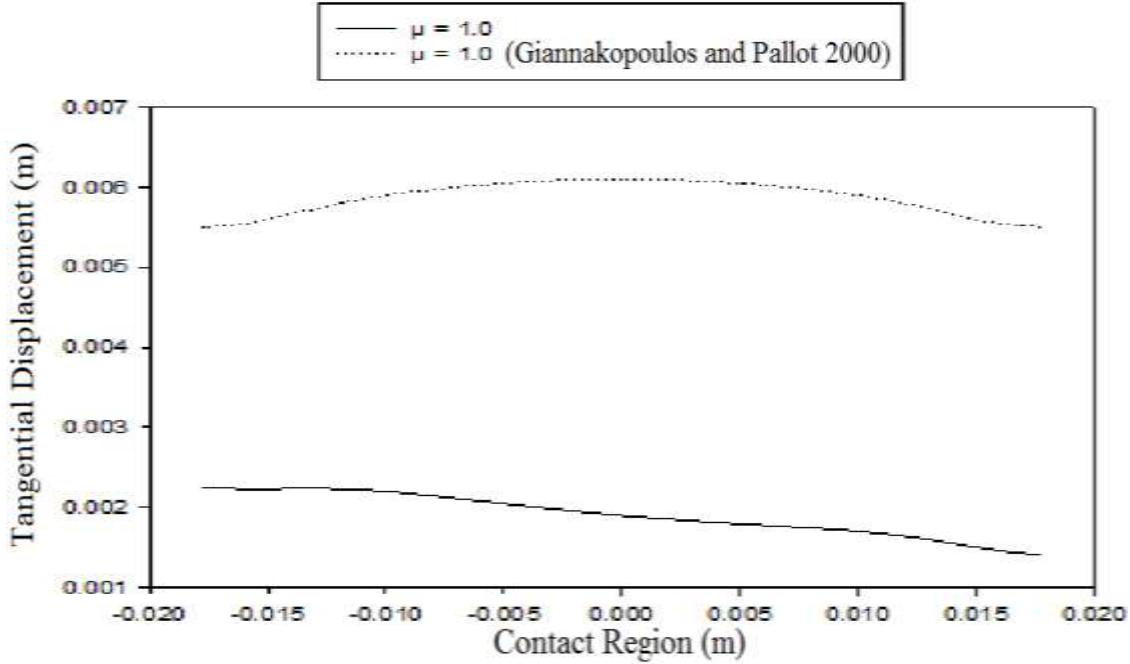


**Figure 11.** The comparison of the tangential displacement between the Giannakopoulos and Pallot’s method and the method that is used in this study.

By substituting the amounts of  $s_{xx}$  and  $s_{yy}$  in the Equation 27 and applying partial integral solution method to solve the normal displacement integral equation, Equation 30 is obtained.

$$u_s(x) = \frac{(1-\nu^2)\beta \cos(\beta\pi/2)}{E_s(k+1)k2J_s} + \left( \frac{q(s)(x-s)^{-k+1}}{-k+1} - \frac{(\partial q(s)/\partial s)(x-s)^{-k+2}}{(-k+1)(-k+2)} + \frac{(\partial^2 q(s)/\partial s^2)(x-s)^{-k+3}}{(-k+1)(-k+2)(-k+3)} \right)_a^x + \left( \frac{q(s)(s-x)^{-k+1}}{-k+1} - \frac{(\partial q(s)/\partial s)(s-x)^{-k+2}}{(-k+1)(-k+2)} + \frac{(\partial^2 q(s)/\partial s^2)(s-x)^{-k+3}}{(-k+1)(-k+2)(-k+3)} \right)_x^a + \frac{(1-\nu^2)\beta \sin(\beta\pi/2)}{E_s(k+1)k2J_s} + \left( \frac{p(s)|x-s|^{-k+1}}{-k+1} - \frac{(\partial p(s)/\partial s)|x-s|^{-k+2}}{(-k+1)(-k+2)} + \frac{(\partial^2 p(s)/\partial s^2)|x-s|^{-k+3}}{(-k+1)(-k+2)(-k+3)} \right)_a^x \quad (30)$$

Moreover, Equation 30 is equal to

$$+ \frac{(1-\nu^2)\beta \sin(\beta\pi/2)}{E_s(k+1)k2J_s} + \left( \frac{p(a)|x-a|^{-k+1}}{-k+1} - \frac{(\partial p(a)/\partial s)|x-a|^{-k+2}}{(-k+1)(-k+2)} + \frac{(\partial^2 p(a)/\partial s^2)|x-a|^{-k+3}}{(-k+1)(-k+2)(-k+3)} \right) - \left( \frac{p(-a)|x+a|^{-k+1}}{-k+1} - \frac{(\partial p(-a)/\partial s)|x+a|^{-k+2}}{(-k+1)(-k+2)} + \frac{(\partial^2 p(-a)/\partial s^2)|x+a|^{-k+3}}{(-k+1)(-k+2)(-k+3)} \right) \quad (31)$$

By applying the following equation, the tangential displacement inside the slip region of contact zone can be obtained. However, Equation 32 is not dependent on stress, but the method that is used in this study to obtain displacement is dependent on normal and tangential stress. By using the following equation, the results of the method that is used in this research is compared with the results obtained by Equation 32 (Giannakopoulos and Pallot, 2000). In

Figure 11, the comparison of the tangential displacement between the Giannakopoulos and Pallot’s method and the method that is used in this study is illustrated.

$$u_s(x) = \mu \frac{(k+1)(1-\nu)h(a^2 - kx^2)}{1 - (k+1)\nu a^2} \quad (32)$$

Figure 10 illustrates the tangential displacement inside the contact region of rigid cylinder with substrate (Giannakopoulos and Pallot 2000).

## RESULTS AND DISCUSSION

Table 2 indicates the comparison of numerical values of points 1 to 12 between Muskhelishvili’s closed-form expression (Hills et al., 1993) and Figure 7 (The analytical method that is used in this study). These figures show the tangential stress in unit of length in partial slip contact region. A comparison of the results of Figures 4 and 8 indicated in Table 2 obviously revealed that the results in most of the coordinates are similar whereas in some coordinates are identical. Therefore, by considering a proper safety factor, the results of this study can be used to obtain stress inside the contact region and to design contacting materials in many mechanical processes.

Obviously, according to Table 3, the numerical results obtained from this study have lower numerical amounts in comparison with results obtained from Giannakopoulos and Pallot’s method. It can be concluded that the

**Table 2.** Coordinates of points 1 to 12 in Muskhelishvili's closed-form expression and Figure 7.

Model	Coordinates (x, y)	Point 1	Point 2	Point 3	Point 4	Point 5	Point 6	Point 7	Point 8	Point 9	Point 10	Point 11	Point 12
Muskhelishvili's closed-form expression	X	-1	-0.85	-0.68	-0.5	0	0.5	0.68	0.85	1	0	0	0
	Y	0	0.47	0.7	0.86	1	0.875	0.71	0.49	0	0.13	0.3	0.5
Figure 7	X	-1	-0.875	-0.72	-0.5	0	0.5	0.72	0.875	1	0	0	0
	Y	0	0.41	0.72	0.93	1	0.93	0.72	0.41	0	0.25	0.5	0.75

**Table 3.** The comparison of the tangential displacement numerical values inside the contact region between the Giannakopoulos and Pallot's method and the method that is used in this study.

Analytical methods Contact region (m)	Numerical values of the tangential displacement inside the contact region at $\mu = 1$ (m)	
	Giannakopoulos and Pallot's method	The method that is used in this study
X = - 0.0178	0.0055	0.00225
X = - 0.0100	0.0059	0.00220
X = 0.0000	0.0061	0.00190
X = 0.0100	0.0059	0.00170
X = 0.0178	0.0055	0.00140

difference between the results is due to the fact that in this study, only the first two terms of partial integrals solution is considered, but in Giannakopoulos and Pallot's method, the whole integral equation is used to obtain the results.

**Conclusions**

One of the important results achieved in this research is that, in slip region, it seems that with increasing friction coefficient, tangential stress and shear stress are increased, but normal stress in almost all of contact zone is constant. The figure of tangential stress (Figure 7) inside the contact region is symmetrical because the numerical values of tangential stress in both

posterior and anterior halves of the contact region are equal. In addition, the figure of shear stress (Figure 6) and especially the normal stress (Figure 5) are asymmetrical because in posterior half of the contact region numerical values are greater than in the anterior half of the contact region. It appears that by increasing the friction coefficient, the tangential and normal displacements are increased. The figure of tangential displacement (Figure 8) inside the contact region is asymmetrical because the numerical values of tangential displacement in posterior half of the contact region are greater than anterior half of the contact region. The figure of normal displacement (Figure 9) inside the contact region is symmetrical because the numerical values of normal displacement in both

posterior and anterior halves of the contact region are equal.

Applications of the present research are broad in the field of contact mechanics; the contact of tire with road and the contact of wheel with rail, and so on. By identifying the effect of friction on stress and displacement fields inside the contact region, the design can be done by an appropriate safety factor. In circumstances that a high friction can make the stress or displacement to pass the valid numerical value of design, decreasing the friction coefficient by selecting the materials with proper numerical values of friction coefficient in order to decrease the numerical values of the stress and displacement is possible. For the future work, the investigation of friction coefficient as a function of time inside the contact region is

proposed.

## CONFLICT OF INTERESTS

The authors have not declared any conflict of interests.

## ACKNOWLEDGMENTS

The author would like to appreciate the guidance of advisors. All the funding related to this research is provided by the presented author.

## REFERENCES

- Anvari A (2014). Fatigue life prediction of unidirectional carbon fiber/epoxy composite in Earth orbit. *Int. J. Appl. Math. Mech.* 10(5):58-85.
- Anvari A (2016a). Fatigue life of unidirectional carbon fiber/epoxy in Earth orbit and Mars. 33<sup>rd</sup> annual RCAF conference, University of Missouri-Columbia, U.S.A.
- Anvari A (2016b). Friction coefficient variation with sliding velocity in copper with copper contact. *Period. Polytechnica, Mech. Eng.* 60(3):137.
- Anvari A (2017). Crack growth as a function of temperature variation in carbon fiber/epoxy. *J. Chem. Eng. Mat. Sci.* 8(3):17-30.
- Anvari A (2017a). Effect of nano carbon percentage on properties of composite materials. *J. Chem. Eng. Mat. Sci.* 8(4):31-36.
- Anvari A (2017b). Failure of Nickel-base super alloy (ME3) in aerospace gas turbine engines. *J. Chem. Eng. Mat. Sci. Under Press.*
- Anvari, A (2017c). "Fatigue life prediction of unidirectional carbon/fiber epoxy composite on Mars. *J. Chem. Eng. Mat. Sci. Under Press.*
- Areias P, Pinto da Costa A (2014). An alternative formulation for quasi-static frictional and cohesive contact problems. *Comp. Mech.* 53:807-824.
- Areias P, Rabczuk T, Queiros de Melo FJM, Cesar de Sa J (2015). Coulomb frictional contact by explicit projection in the cone for finite displacement quasi-static problems. *Computat. Mech.* 55(1):57-72.
- Carter FW (1926). On the action of a locomotive driving wheel. *Proceedings of the Royal Society of London, London*, pp. 151-157.
- Galin LA (1953). Contact problem of the theory of elasticity. (I.R.) *Gostekhizdat, Moscow* pp. 4-272.
- Giannakopoulos AE, Pallot P (2000). Two - dimensional contact analysis of elastic graded materials. *J. Mech. Phys. Solids* 48(8):1597-1631.
- Goryacheva IG (1998). *Contact Mechanic in Tribology*. Kluwer Academic Publishers - Dordrecht / Boston / London, Netherlands.
- Guler MA, Adibnazari S, Alinia Y (2011). Tractive rolling contact mechanics of graded coatings. *Int. J. Solids Struct.* 49(6):929-945.
- Haines DJ, Ollerton E (1963). Contact stress distribution on elliptical contact surfaces subjected to radial and tangential forces. *Proc. of Inst. Mech. Eng. London* pp. 45-54.
- Hertz HR (1882). *Miscellaneous Papers*. London: Macmillan & Co, 1896. Cap. 5 – On the contact of two elastic solids. Eight's Edition.
- Hills DA, Nowell D, Sackfield A (1993). *Mechanics of Elastic Contacts*. Butterworth–Heinemann, Oxford.
- Johnson KL (1958). The effect of a tangential contact force upon the rolling motion of an elastic sphere on a plane. *J. Appl. Mech.* 25:339-346.
- Kalandiya AI (1975). *Mathematical methods of two-dimensional elasticity*. Mir, Moscow pp. 5-290.
- Kalker JJ (1967). On the rolling contact of two elastic bodies in the presence of dry friction. Ph.D. thesis, Department of mechanical engineering, Delft University of Technology.
- Ke LL, Wang YS (2010). Fretting contact of two dissimilar elastic bodies with functionally graded coatings. *Mech. Adv. Mater. Struct.* 17:433-447.
- Li Z, Kalker JJ (1998). The computation of wheel-rail conformal contact. *computational mechanics, new trends and applications*, S. Idelsohn, E Onate and E Dvorkin (Eds), CIMME, Barcelona, Spain.
- Muskhelishvili NI (1949). *Some basic problems of the mathematical theory of elasticity*. (I.R.) Nauka, Moscow. Third Edition.
- M'ewen E (1949). Stresses in elastic cylinders in contact along a generatrix. *Philosophical Magazine, Cambridge* 40:454-459.
- Ruderman M, Bertram T (2011). Modified Maxwell-slip Model of Presliding Friction. Institute of Control Theory and Systems Engineering (RST), Technische Universitat (TU) Dortmund, 44221-Dortmund, Germany.
- Sackfield A, Hills DA (1983). Some useful results in the classical Hertz contact problem. *J. strain Anal.* London 18(2):101-105.
- Santos FdC, Santos AAd, Bruni JrF, and Santos LT (2004). Evaluation of Subsurface Contact Stresses in Railroad Wheels Using an Elastic Half-Space Model. Department of mechanical design, Campinas, SP. Brazil 13083-13970.
- Steen R (2010). Enhanced friction modeling for steady - state rolling tires. Ph.D. thesis, Eindhoven University of Technology, Eindhoven, the Netherlands.
- Timon R, Huilong R (2017). A peridynamics formulation for quasi-static fracture and contact in rock. *Eng. Geol.* 225C:42-48.
- Vermeulen PJ, Johnson KL (1964). Contact of non-spherical bodies transmitting tangential forces. *J. Appl. Mech.* 31:338-340.